Development of image analysis pipeline to investigate the impact of microplastic to bacterial aggregation

Bachelor thesis

Student: Karoline Lindpere
Supervisor: Simona Bartkova, researcher at DCB
Co-supervisor: Ott Scheler, associate professor at DCB
Study program: LAAB

Tallinn 2024

Pildianalüüsi töövoo arendamine mikroplastiku mõju uurimiseks bakterite agregatsioonile

Bakalaureusetöö

Üliõpilane: Karoline Lindpere
Üliõpilaskood: 212999LAAB
Juhendaja: Simona Bartkova, KBI teadur
Kaasjuhendaja: Ott Scheler, kaasprofessor
Õppekava: LAAB

Tallinn 2024

Declaration

Hereby I declare that I have compiled the paper independently and all works, important standpoints and data by other authors have been properly referenced and the same paper has not been previously been presented for grading.

Author: Karoline Lindpere
(Digitally signed)

The paper conforms to requirements in force.
Supervisor: Simona Bartkova
(Digitally signed)

Permitted to the defence.
Chairman of the Defence Committee:

Abbreviations

o/w – oil in water
w/o – water in oil
w/o/w – water-oil-water
o/w/o – oil-water-oil
PCR – Polymerase Chain Reaction
DNA – Deoxyribonucleic acid
CRISPR – Clustered Regularly Interspaced Short Palindromic Repeats
PddCas – Polydisperse Droplet Digital CRISPR/Cas
RNA – Ribonucleic acid
SARS-CoV-2 – Severe Acute Respiratory Syndrome Coronavirus 2
HPV 18 – Human Papillomavirus type 18
ddIA – Digital Droplet Immunoassay
DAPI – 4',6-diamidino-2-phenylindole
CCM – cerebral cavernous malformation
IgA – Immunoglobulin A
GFP – Green Fluorescent Protein
AMR – Antimicrobial resistance
rRNA – ribosomal RNA
IPC – Imperial Privy Council
DIC – Differential Interference Contrast
E. coli – *Escherichia coli*
MP – microplastic
CP – CellProfiler™

Table of Contents

INTRODUCTION

Droplet emulsions consist of dispersed and continuous phase mixtures. They can be made with microfluidics to create monodisperse droplets or by shaking to create polydisperse droplets. Microfluidics usually needs expensive equipment and special training of users, while polydisperse droplets can be done in any lab without equipment nor specialized training.

One way droplets can be analysed is via imaging using a microscope. For image analysis, there have been developed many software. Most of them require programming skills or cost money. However, there are also software available, which are free of charge and user-friendly, meaning no programming skills are needed. These software have their own communities, which constantly strive to improve and broaden the scope of the software applications.

One of the major problems currently in the world is currently plastic waste. The plastic can break down into microplastic and nanoplastic, which are a threat to our health and ecosystem. Microplastic can function as a surface for bacteria to form aggregates, eventually leading to biofilm formation. This concern has gone so far that we now have microplastic based ecosystems, called plastispheres. These systems are ideal places for microbes to form biofilm, thus endorsing antimicrobial resistance.

The aim of this thesis is to investigate the impact of microplastic to bacterial aggregation. The methodology includes developing a pipeline in software CellProfiler™ in combination with software ilastik, to (i) detect microplastics, (ii) improve polydisperse droplet detection, and (iii) divide droplets based on their pixel texture into three groups: no growth, homogeneous growth and aggregated growth.

The theoretical part presents an overview of droplet emulsion and commonly used software for image analysis, with focus on open-source ones. For the last part, it describes microplastic, antimicrobial resistance and biofilm. The methods and materials chapter includes the steps for developing the pipeline in CellProfiler™ and ilastik and explains how the used software work. In the last chapter, all the results about the developed pipeline are described in detail. This section highlights, how droplet detection has been optimized in CellProfiler™ and how microplastics are identified in ilastik. Additionally, it compares the bacterial viability and autoaggregation in polydisperse droplets with and without microplastics.

1. LITERATURE OVERVIEW

1.1 Droplet emulsion

Emulsions are mixtures of two immiscible liquid phases – discontinuous phase, also called internal phase, and continuous phase, also called external phase [1]. Although emulsion is a weak system, it can be stabilized with an emulsifier, also called the interphase between the two other phases. Emulsions can be classified based on the dispersed phase or the size of the droplets [1]. Types of emulsion based on dispersed phase are oil in water (o/w), water in oil (w/o) or multiple emulsion (w/o/w or o/w/o) (**Figure 1**)**.** Droplets with sizes up to 0.2 micrometer are called microemulsion, 0.2 to 50 micrometer are called macroemulsion and 50 to 1000 nanometer are called nanoemulsion [1]. It is a way to do small–scale experiments, which have many advantages – the cost of the reagents is lower and the toxic waste decreases [2].

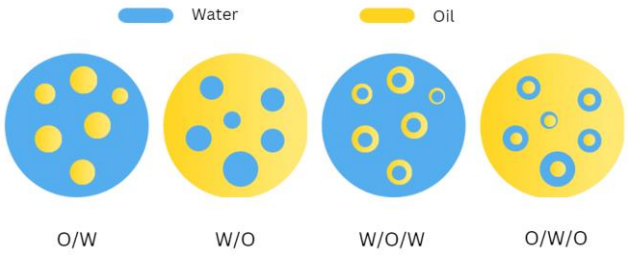

Figure 1. Types of emulsion based on dispersed phase. From left: oil in water, water in oil, water-oil-water and oil-water-oil.

Droplet microfluidics has made an impact on single cell research. The droplets function as chambers for cell cultures, while providing everything needed for successful cell growth. The microenvironment is easily controllable and by external intervention, the single cell can be simply manipulated. It is possible to observe immediate single – cell activity of enzyme, antibody, or rare cell screening [3]. Another large-scale usage of droplet microfluidics is drug screening, where millions of small compounds need to be filtered. For testing drugs such as antiviral antibodies and antibiotics, droplet-based flows are more frequently used. Despite making gradient determination more challenging, droplet-based flows can regulate sample distribution and duration of residence [2]. The droplets can be produced through microfluidics or bulk solution approaches, where polydisperse droplets are prepared more simpler way [4].

1.1.1 Monodisperse droplets

Monodisperse droplets mean that they all have the same size [5]. The main benefits of microfluidic systems are their ability to control droplet size and production speed. They are taking over the traditional emulsification techniques, like homogenization or sonication, by executing the experiments in small, isolated volumes [5]. Monodisperse droplets are especially needed for applications such as droplets digital polymerase chain reaction and biochemical analysis [6].

Among the various channel designs, the T-junction, Y-junction, co-flow and flow focused designs are the most frequently used [3].

a) The T-junction is the simplest channel design, where the two phases get into contact at the inlet (**Figure 2.a**). One liquid is formed into droplets within another liquid. If the oil is

connected to the main channel, then it leads to the downstream part of water being squeezed and cut off, effectively generating small droplets (**Figure 2.a**) [3].

b) T-junction design can also work if the channels are reversed. The water phase is cut under pressure (**Figure 2.b**) [3]. The size of droplets depends on channel diameter, flow rate of the fluid or relative viscosity of the phases [7].

c) The Y-type channel is like T-junction, except phases flow from an angle (**Figure 2.c**) [3].

d) Co-flow design includes two concentric channels from which the inner one usually has a pointed tip. The droplets are formed due to the interfacial tension being surpassed by the viscous resistance, created by the oil phase (**Figure 2.d**) [3].

e) Flow focusing design is similar to co-flow design as it also includes two concentric channels from which the inner one usually has a pointed tip [3]. The faster the flow rate of the external phase, the smaller the forming droplets [7]. The flow-focusing design incorporates an additional narrow channel into the main flow channel (**Figure 2.e**) [3].

f) Cross-focusing flow design is the newest design, where the oil phase flows through two channels and parts the water phase at the crossroad (**Figure 2.f**) [3].

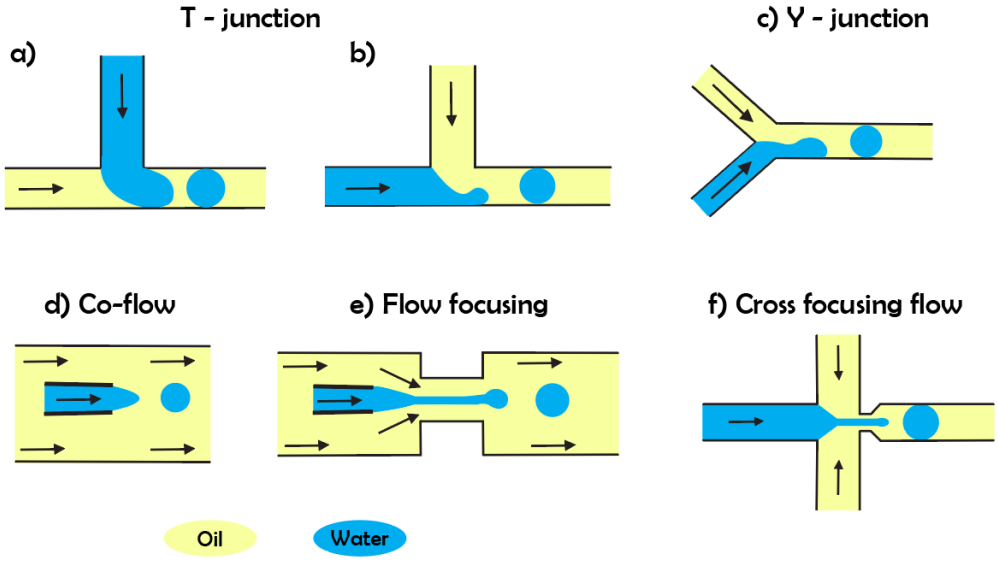

Figure 2. Different channel designs. T-junction is the easiest design (a,b). a) Water is being squeezed, which cuts water phase into droplets. b) Droplets are formed due to pressure from oil phase. c) Y – junction, where both phases flow from an angle. d) Co-flow and e) flow focusing designs are more complicated, which include inner channel with pointed tip. f) Cross focusing flow, the newest design, where the oil phase pushes against the water phase, thus generating droplets.

Although lab-on-a-chip has had great improvement, one of the downsides of microfluidics is the need for expensive equipment and trained staff [4].

1.1.2 Polydisperse droplets

To overcome the restrictions of using microfluidics, an alternative possibility is to generate polydisperse droplets instead. Generation of polydisperse droplets does not require any need for unique equipment, so it can be done in any standard laboratory. These droplets are made by shaking with a hand or vortexed, so the two phases would mix and generate droplets. Since there is no special equipment, the droplet sizes vary, which depend on the viscosity ratio of the dispersed and continuous phases (**Figure 3**) [4], [8].

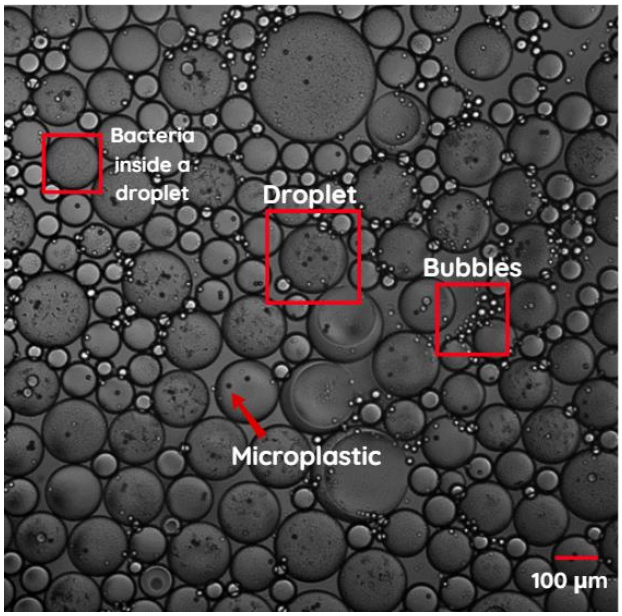

Figure 3. Example of water-in-oil polydisperse droplets from MSc thesis made by Fenella Lucia Sulp [37]. Droplets are able to contain bacteria and microplastic if needed. On the other hand, bubbles are byproducts of producing droplets when shaking. They are too small to contain anything.

Polydisperse droplets can be used in many different biological assays, which will make the process simpler while still giving accurate results.

Polymerase chain reaction (PCR) has proved to be highly sensitive and can detect specific diseases, which means more precise diagnosis and treatment [9]. There has been developed methods to separate single biomolecules to droplets, but to make it more suitable for everyone (which means no special training or expensive equipment), there is now an opportunity to execute droplet PCR in polydisperse droplets. The polydisperse method adapts to different input sample volumes and takes less time, while still accurately identifying the target DNA [9].

For pathogen diagnosis, the rising technology has been CRISPR – based assays and now there has been developed polydisperse droplet digital CRISPR-Cas-based assay (PddCas). To spot viral DNA/RNA, this method requires only a vortex mixer, and it has higher sensitivity than analogous bulk CRISPR assays. PddCas identified well SARS-CoV-2 and HPV 18, which shows its capability [10].

Another way to detect diseases is through protein detection, for which immunoassays are vital [8]. The polydisperse digital droplet immunoassay (ddIA) does not need any wash steps and the process requires only one reagent addition step, which makes the whole system simpler. Benefits of polydisperse ddIA include sensitivity, cost efficiency and better suitability, since it is applicable for laboratories and also near-patient tests [8].

1.2 Commonly used software for image analysis

There have been many image analysis software developed, but most of them expect skills in programming, such as MATLAB, or are more user-friendly, but only monetarily accessible, such as Zen [11]. Having free of charge and easily operated image analysis software is a high demand. Such

most popular software are CellProfiler™, ilastik, ImageJ, and QuPath. These four can be divided into two groups considering their workflow. CellProfiler™ and ImageJ belong to the rule-based software group. This means that software need settings to detect objects, which are manually provided. Qupath and ilastik are in the machine learning-based group, in which wanted objects are manually highlighted [11].

Table 1. Comparison of different widely available software [11].

Software	Price	Batch processing	Batch processing time, 64 images (in seconds)	Accuracy	Precision
CellProfiler™	Free	No extra programming steps	873.86 ± 15.42	96.2%	99.8%
ilastik	Free	No extra programming steps	1081.59 ± 15.48	74.7%	80.2%
QuPath	Free	Extra process and scripting	55.96 ± 3.60	80.9%	83.1%
ImageJ	Free	Extra process and scripting	91.10 ± 0.97	92.7%	96.3%

In this study two software were used - CellProfiler™ and ilastik. Of these four software, CellProfiler™ had the highest accuracy (96.2%) and precision (99.8%). CellProfiler™ and ilastik are from these four software more convenient for batch analysis [11]. Having user-friendly way to do batch analysis is vital, since droplet-based experiments generate thousands of droplets that need to analyzed.

1.2.1 Cellprofiler™

CellProfiler™, open-source image analysis software, was first introduced in 2005 [12]. It is designed for biologists [13], while keeping in mind their low skills in programming [11]. Needing no special training, users can analyse their images using modular processing pipelines. There is a wide range of built-in modules, which can be turned into various pipelines, depending on the desired analysis. CellProfiler™ gets constantly improved from feedback from biologists. For CellProfiler™ 4.0, the goal was to make it more accessible and even easier for developing pipelines [12].

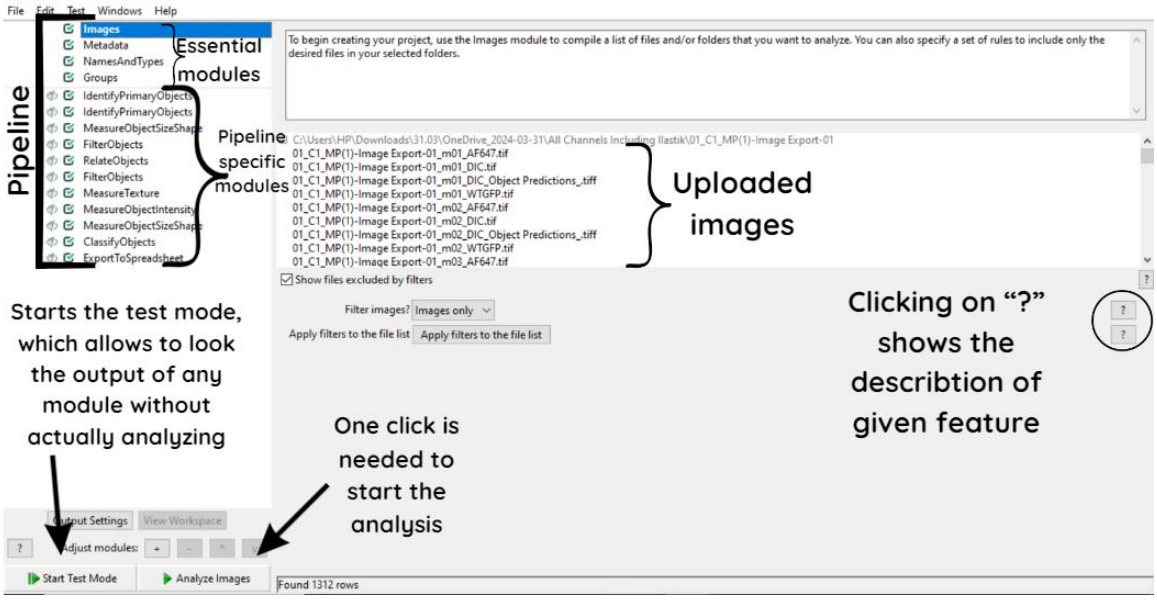

Figure 4. How the first module Images look in CellProfiler™. On the left is pipeline with essential modules on top, followed by modifiable modules. Remaining space is for the module features.

The concept of how to operate the software is straightforward. First a pipeline, series of image-processing modules, is needed. Then, considering the characteristics of analyte, settings must be adjusted. After everything is set, images can be processed automatically. Lastly, the data will be exported to a spreadsheet (**Figure 4**) [13]. Another benefit of using CellProfiler™ is their helpful website, which has step by step guide how to get started, tutorials, manuals of every version and even examples of pipelines with images. Over time it grew its own community and there is a possibility to get help from support forum. People can write their issues and get help and/or advice [13].

CellProfiler™ has been used in numerous studies:

1. During the study by Simona Bartkova *et al.*, a pipeline was created that successfully identified droplets and measured fluorescence intensity of these droplets. In total the pipeline analyzed thousands of droplets [14].
2. During the study by Yeh Siang Lau *et al.*, the MuscleAnalyzer pipeline was created. This pipeline analyzed laminin and DAPI co-stained muscle images, giving quantitative measurements for muscle histological properties [15].
3. CellProfiler™ was used by researchers at the University of Utah to uncover image-based traits connected to a monogenic rare disease, the hereditary stroke syndrome cerebral cavernous malformation (CCM) [13].

1.2.2 ilastik

One o currently popular supervised machine-learning-based software is ilastik. It is an interactive tool with many pre-defined workflows, such as pixel classification or object classification [16]. The software learns from labels provided by the user and once it has been trained, the data can be applied in batch processing. Of course, ilastik too has its own limits, such as colour and texture, but for general image analysis in different scientific fields, it produces quality results if supervised appropriately [17].

The most popular workflow is pixel classification, which connects every pixel of an image to a label, which is defined by the user. Label may stand for example microplastic or background. The user must mark parts of the image under the right label. To do that, there are different coloured brushes. After the training, software probabilities are calculated and all the pixels are assigned to given labels [16]. As pixel classification cannot recognize characteristics of an object, such as shape, there is another workflow for that part. Object classification is similar to pixel classification, but it goes more into detail, as it needs e.g. smoothing and thresholding [16]. There are also detailed guidelines for getting started or descriptions of all the available workflows on the website. Additionally, there is a possibility to report a problem or give a suggestion for new features [18].

Example studies, where ilastik was used:

1. During the study by Kathrin Moor *et al.* about high-avidity IgA, cells from caecal content were categorized into red (mCherry+) and green (GFP+) types [19].
2. During the study by William Menegas *et al.*, ilastik was used to identify cell and non-cell pixels. In total there were eight different algorithms that were trained by hand [20].

1.3 Microplastic and its influence on antimicrobial resistance (AMR) and aggregation

Plastic waste is a pollutant that is everywhere and thus closely tied to our daily lives. Microplastics are fractions of plastic waste, which usually comes from decomposition of larger plastic debris. The particles are smaller than 5 mm [21]. The global plastic production has had a massive increase with Asian countries in the lead. Most of the waste is being dropped into the environment. Microplastic pollution has been turned into a major concern for human health due to finding particles in biological samples, such as saliva and blood [22].

Another global health treat is antimicrobial resistance (AMR). Such pollutants as antibiotics or heavy metals are helping antibiotic resistant bacteria to develop and persist in the environment [23]. It is related to outspread abuse of antibiotics across various areas [24].

1.3.1 Nano- and microplastic

Plastic is not biodegradable, it just breaks down into smaller fragments such as microplastic or nanoplastic. Fragment sizes 0.1 µm to 5 mm are categorized as microplastic and fragments smaller than 0.1 µm fall into nanoplastic category [23]. Although plastic as a material is relatively new, the extreme production and use has led to it being a risk to the environment [22].

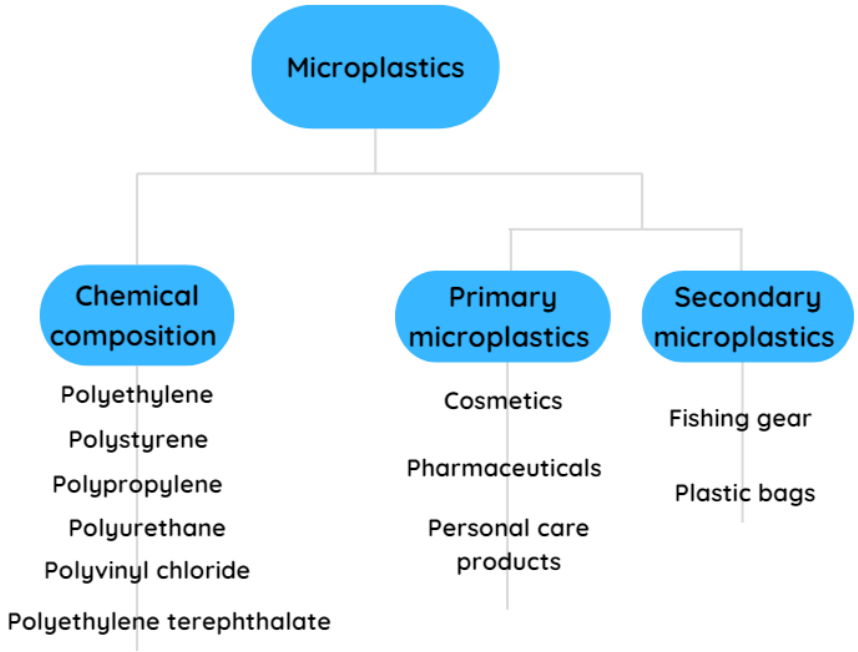

Figure 5. Different ways to categorize microplastics. Microplastics can be categorized according to their chemical composition or whether it is a primary or a secondary microplastic. Primary microplastics are intentionally added to products while the forming of secondary microplastics is unpredictable

Microplastics can be divided into two classes. Primary microplastics are deliberately made small and included into consumer and commercial products, for example cosmetics, pharmaceuticals, and personal care products. Secondary microplastics, for example fishing gear or plastic bags, are formed involuntarily [22]. Breakdown of larger polymers is a result of physical, chemical, or

biological factors. Another way for classifying microplastics is to divide them into five types: fragments, fibres, foam, pellets, and films. Furthermore, it is possible to sort them according to their chemical composition: polyethylene, polystyrene, polypropylene, polyurethane, polyvinyl chloride, and polyethylene terephthalate (**Figure 5**) [22].

It is predicted that humans consume 0.1 - 5 g microplastics each week. The particles can be detected in human feces, blood, lungs, and placentas [25]. Primarily cellular and molecular components of living organisms are damaged by microplastic [22]. Consuming food that has plastic particles in it can lead to inflammatory, pulmonary, and infectious diseases. If the particles have reached the circulatory system, they have easy access to other organs. The toxic components are extracted from plastic particles and cause harm to the human body [25]. It is important to raise awareness already at school, so children can learn about this issue from early on. Also, media has a significant part of educating everyone as well. Releasing documentaries and television shows presenting the issue in a simply understandable way, it supports the public to be more conscious and make better choices [22].

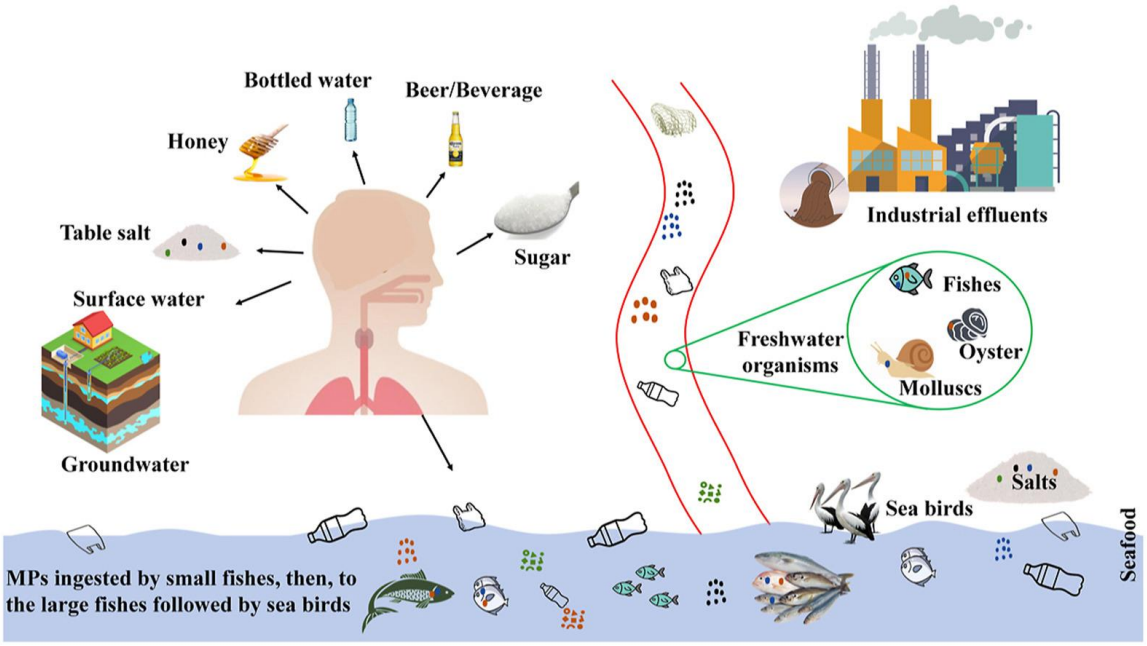

Figure 6. Cycle of plastic consumption. Humans produce plastic products that end up in water. First, small fishes ingest the microplastic particles, then smaller fishes are eaten by larger fishes followed sea birds etc. Humans go fishing and when eating the caught fish, the same particles end up in their system, which causes harm [29].

Even more dangerous than microplastic, may be nanoplastic, since they are more reactive. Due to their smaller size, the particles can extend further and invade more living cells. They connect to the microbe, enter it and the toxic chemicals leached out from plastics cause toxicity [26]. Most frequent way to get in touch with nanoplastic, is through oral intake, that is by drinking water or consuming materials exposed to nanoplastic. Also, worn out car tires produce particles, which get to the streets and may be inhaled [27]. Nanoplastics, that are ingested through the food chain, have been shown to penetrate the blood-brain barrier, resulting in brain injury to fish [28].

1.3.2 Antimicrobial resistance

Antibiotic resistance (AMR) means that bacteria can avoid the effects of drugs, which makes treatment harder or not possible. AMR is linked to exploitation of antibiotics in humans, agriculture, farming and industry [24]. It is moreover connected to many types of microorganisms, such as fungi, parasites, viruses and bacteria [30].

In the bacterial cell, antibiotics inhibit cell wall synthesis, nucleic acid synthesis and protein synthesis [31]. Cell wall synthesis inhibitors, which are from class β- lactams and Glycopeptides, are used to treat both Gram-negative and Gram-positive infections. The antibiotic resistance comes through a synthesis of penicillin-binding protein 2a, which alters the active site of an enzyme so the antibiotic cannot bind [32]. DNA synthesis inhibitors, such as Ciprofloxacin and Levofloxacin, suppress topoisomerase II and IV, which prevents DNA replication. Resistance is caused by chromosomal mutation that codes for protein targets, which lowers the compatibility between antibiotic and enzyme complex [33]. Protein synthesis inhibitors, like Aminoglycosides, Macrolides and Tetracycline, target processes including initiation, formation of the 70s, and elongation in making polypeptides. Antibiotic resistance happens due to different mechanisms, for instance methylation of 16s rRNA causes resistance to aminoglycosides and modification of 23s rRNA causes resistance to macrolide [34].

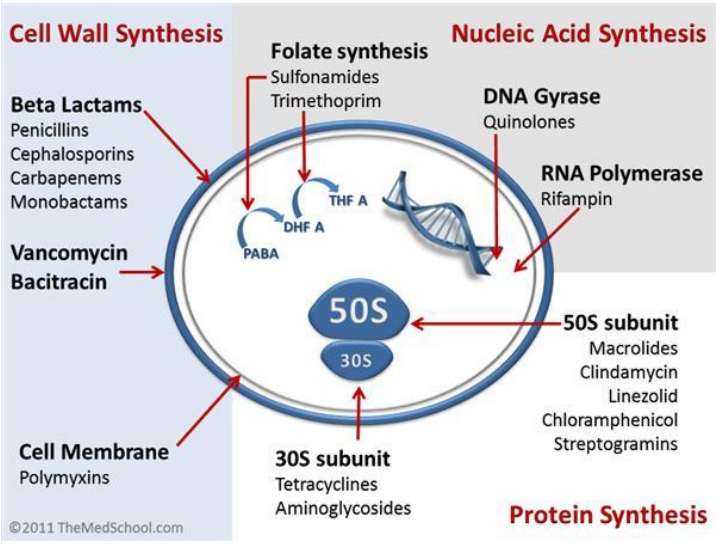

Figure 7. Antibiotic classifications, which inhibit cell wall synthesis, nucleic acid synthesis and protein synthesis [31].

AMR can be intrinsic, acquired and adaptive. Intrinsic resistance describes the resistance that originates from inherent characteristics. For instance, glycopeptide resistance is found in Gram-negative bacteria, conferred by the impermeability of their outer cell membrane. Acquired resistance includes bacteria acquiring resistance through mutations or horizontal gene transfer, which can happen through transformation, transduction or conjugation. Adaptive resistance occurs as feedback from environmental changes. It is an outcome from modulations in gene expression [24].

The correct way to handle AMR in health care is to have reasonable antimicrobial use and high IPC standards. Being a growing problem, AMR needs to be surveyed. The European Antimicrobial Resistance Surveillance Network (EARS-Net) and the Central Asian and European Surveillance of

Antimicrobial Resistance (CAESAR) network are in a close cooperation to collect data from both European Union countries and eastern Europe and central Asia. This helps to have an overview of the AMR situation [30].

1.3.3 Aggregation and biofilms

Biofilms are developed by microorganisms' capability of sticking to surfaces. Depending on the environment, noncellular components, such as mineral crystals or blood components, can also be found in the biofilm matrix (**Figure 7d**). Main composition of biofilms are extracellular polymeric substances (EPS), which can be up to 90% of the total organic carbon [35]. EPS, for instance proteins and nucleic acids, are there to protect microorganisms from photodegradation and physical scrape [26]. Biofilms can develop on a diverse range of surfaces, from living tissues to water system piping [35]. Factors that determine the development of biofilm are water salinity, temperature, and pH [26] Public health is greatly impacted by biofilms, as they cause certain infectious diseases and are common in a variety of device-related infections. Examples of such diseases are cystic fibrosis, otitis media and periodontitis [35].

One of the first steps in forming a biofilm is autoaggregation, which means forming bacterial clumping at the bottom of culture tubes [36]. Aggregating bacteria may get protection from environmental stresses. While autoaggregation specifies that only same strain bacteria associate with each other (**Figure 7b**), aggregation includes any microbial clumpig (**Figure 7a**). There is also co-aggregation, where different bacterial species aggregate (**Figure 7c**) [36].

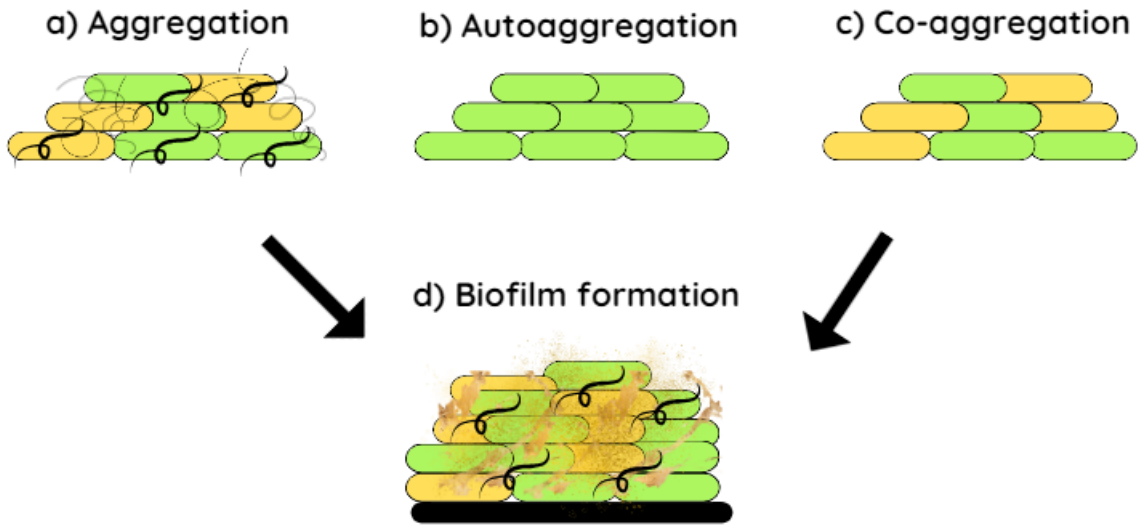

Figure 8. Differences between aggregations. A) Aggregation consists of different particles. B) Autoaggregation is between same strain bacteria. C) Co-aggregation, where different strain bacteria associate with each other. D) In biofilm are also microorganisms and noncellular components. Aggregation can form without a surface, while biofilm forming is more linked with surface.

"Plastisphere" describes microplastic based ecosystems, which have AMR promoting elements. In the plastisphere ecosystems, microbes can attach easier to the chemically and physically altered plastic surfaces. The enduring qualities and surface features of microplastics not only make them

an ideal host for microbes, but also contaminants such as heavy metals and antibiotics, all together making plastispheres very effective AMR promoting environments [23].

2. AIMS OF THE STUDY

The main aim of the thesis was to develop an image analysis pipeline to investigate the impact of microplastic to bacterial aggregation.

The specific sub-aims of this thesis were:

1. Detection of microplastic inside polydisperse droplets
2. Optimizing the detection of polydisperse droplets
3. Comparison of bacterial viability in polydisperse droplets with microplastic versus without microplastic
4. Comparison of bacterial aggregation in polydisperse droplets with microplastic versus without microplastic

3. MATERIALS AND METHODS

This thesis is part of a bigger „ecosystem“ of theses projects in the TalTech Microfluidics group. It is connected to other past, present, and future projects within the group. The author of this thesis is using images from the past MSc thesis of Fenella Lucia Sulp [37] and collaborating partially, during the initial stages, with MSc student Merili Saar. The developed pipeline of this thesis will be used by BSc student Triini Olman, in her own thesis (**Figure 9**).

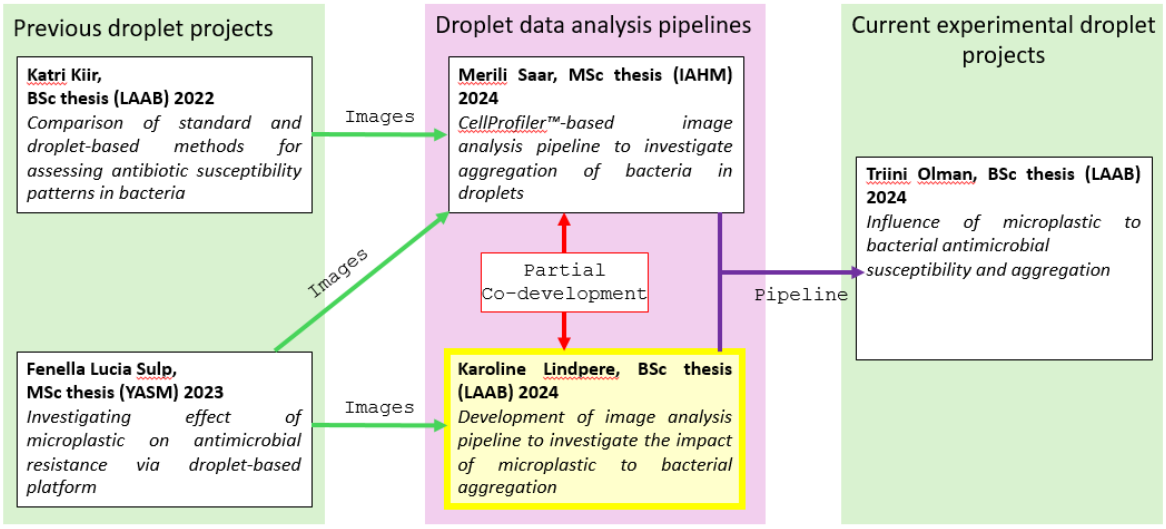

Figure 9. The ecosystem of biofilm and aggregation-related theses in TalTech Microfluidics group.

The MSc thesis of Fenella Lucia Sulp investigated the effect of microplastic on antimicrobial resistance via droplet-based platform. The experimental part consisted of polydisperse droplet generation and microscopy imaging. In short, *Escherichia coli* JEK 1036 with chromosome-incorporated gene encoding the green fluorescence protein (GFP) was mixed with (i) Polystyrene 10 µm microplastic spheres 10% solids (+- 0.5%) in milli-Q Ultrapure water, (ii) Dextran, Alexa Fluor™ 647, 10,000 MW, anionic, fixable (Invitrogen, Life Technologies Corporation), and (iii) nine different concentrations of the antibiotic Cefotaxime (Carbosynth Limited). Polydispersed droplets were generated by adding Novec HFE 7500 fluorocarbon oil with 2% concentration of perfluoropolyether (PFPE)–poly(ethylene glycol) (PEG)–PFPE triblock surfactant (obtained as a gift from Prof. Garstecki, ICHF PAN, Poland) to each sample, followed by vortexing of each sample Eppendorf tube and incubating overnight at 37°C.

Droplets were imaged as a monolayer with LSM 900 Laser Scanning Microscope (Zeiss, Germany) running on ZEN 3.3 (blue edition) software with the following settings:

- Objective Plan-Apochromat 10x (NA 0.45)
- LED light source Colibri 7
- Diode lasers 488 nm and 640 nm
- Green channel: excitation 395 and emission 502
- Red channel: excitation 653 and emissioon 668
- Bright-field channel: DIC

The green channel was used for *E. coli* bacteria, the red channel was for detection of polydisperse droplets and DIC was used for detecting microplastic. In total were 328 images, which were analyzed also in this thesis.

This thesis continues Fenellas's previous work by developing the necessary analysis pipeline for (i) detecting individual microplastic particles inside polydisperse droplets, (ii) optimizing polydisperse droplet detection, and (iii) analysing bacterial growth (possible autoaggregation). This will enable taking a deeper look into the relationship between microplastic and possible bacterial aggregation pattern for future studies.

3.1 Detection of microplastic

An important part of this thesis was detecting microplastic particles in polydisperse droplets, which was done using the software ilastik (version 1.4.0.post1). The main idea of using ilastik is to train the software to find what is needed, which in this case are microplastic particles inside polydisperse droplets.

1) *Input data* - The first step is to upload training images. In this study, 3 representative images were chosen – two from control sample without any antibiotic present and one from sample with Cefotaxime concentration of 0.008.
2) *Feature selection* – this module determines how the different classes of pixels will be distinguished in the next steps. ilastik provides three features, which are colour/intensity, edge, and texture. The scales correspond to the sigma of the Gaussian used to smooth the image before applying the filter. Larger sigma gets information from larger area but balances out the details.
3) *Training* – In this module are two labels. One is for identifying needed objects, and the other one is marking everything else that could disturb the classification, for example outline of droplets. In this study the objects were microplastic particles and the main disturbance came from small, similar in size bubbles that often arise during polydisperse droplet generation (**Figure 10**).
4) *Thresholding* - First there is a choice between the simple and hysteresis method. Simple method means that thresholding will be done at one level, whereas hysteresis method performs it at two levels – first high threshold and then low threshold. This method makes it possible to separate connected objects and selects objects that have high probability. To find the best threshold, different values were tested – the automatic value for smoothing was one, so it was tested with 0.5 increments below and above one to see possible improvement in detection. The tested smoothing values, which will reduce noise, were different combinations of 1, 1.5 and 2. The tested threshold values stayed between 0.9 - 0.5.
5) *Object classification* – ilastik shows what it has identified, but there still could be some errors. For this reason, there are again the two labels from training module with the possibility to mark correctly and incorrectly identified objects. If needed, there is a possibility to go back to training module for further training.

6) *Object information export* – The pixel values range in every channel from 0.0 to 1.0, which show the probability that a pixel belongs into a certain class. In the end, there are two probabilities exported – one channel per label class.

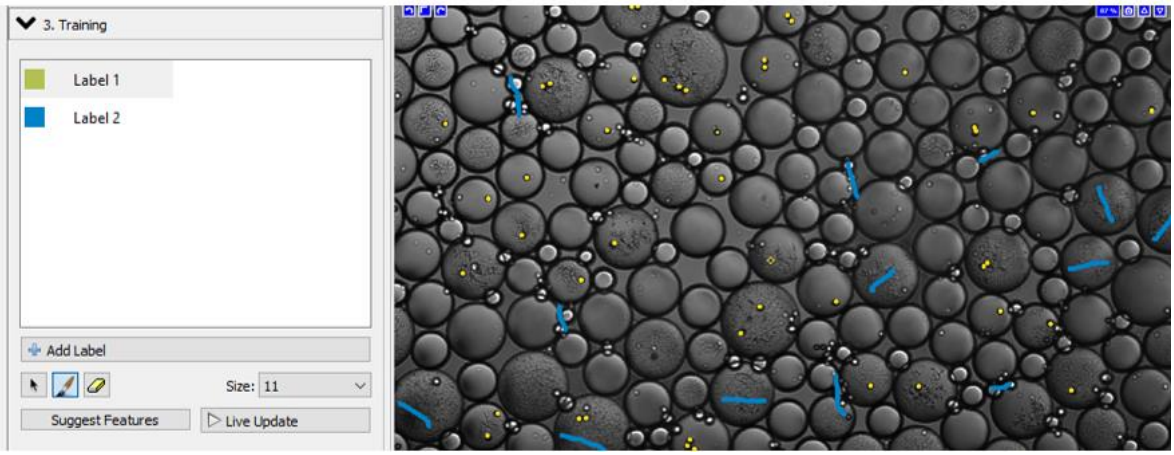

Figure 10. Training module in ilastik. Microplastics are marked with label one (yellow color) and other disturbing factors, for example small bubbles or bacteria, are marked with label two (blue color).

To identify microplastic inside polydisperse droplets, an additional *IdentifyPrimaryObjects* module is then added in the CellProfiler™ (version 4.2.6) pipeline, which uses the binary output probability tiff files from ilastik as input files.

To make sure that ilastik was well trained, accuracy was calculated using formula in **Figure 11**.
In this case:

1) True positive (TP) – there is microplastic and ilastik finds it
2) False negative (FN) – there is microplastic, but ilastik cannot find it
3) False positive (FP) – there is no microplastic, but ilastik counts something as microplastic
4) True negative (TN) – there is droplet with no microplastic and ilastik does not find anything

$$\text{Accuracy} = \frac{TP + TN}{TP + FP + TN + FN}$$

Figure 11. Formula to calculate accuracy.

3.2 Optimizing droplet detection in CellProfiler™

CellProfiler™ contains four essential modules that are automatically included in any pipeline. The essential modules define how the images are organized for analysis.

Essential modules:

1) *Images* – allows to drop files and/or folders that need to be analysed
2) *Metadata* – allows to extract information, which will be stored with the measurements
3) *NamesAndTypes* – allows to name each image by which upcoming modules will refer to
4) *Groups* – allows the list of images to be divided into subsets which will be processed separately of each other

For further analysis of specific images, additional modules are added, and settings adjusted to develop an optimal analysis pipeline. Prior analysis pipeline used in the MSc thesis by Fenella Lucia Sulp was therefore significantly modified in this thesis. For optimizing polydisperse droplet detection, emphasis was placed to specific settings in *IdentifyPrimaryObjects* module.

Diameter of objects

One of the modified module features was the maximum and minimum diameter of objects in pixels to know what to count as a droplet and what to discard. These numbers were found by manually measuring the smallest and biggest droplet diameter of 19 images (**Appendix 2**). Fenella Lucia Sulp had 19 folders of images, each folder containing 40 different images, which brings the total amount to 760 droplet images. From these folders 1-9 contained images with microplastic particles and folders 11-19 images without microplastic particles. Folders 1-9 and 11-19 contained different antibiotic concentrations - 0.075, 0.056, 0.042, 0.032, 0.024, 0.018, 0.013, 0.010, 0.008 µg/mL. Folder number 10 was control. All the images were picked randomly.

Thresholding

Another important part of *IdentifyPrimaryObjects* module is threshold. Determining the right smoothing scale and correction factor is needed for the best results. Threshold smoothing scale smooths the image before the threshold is applied, for example removing holes. Threshold correction factor adjusts the threshold by multiplying it by this value. Value between 0 and 1 makes the threshold more lenient, value of 1 makes no adjustments and value higher than 1 makes the threshold stricter.

Smoothing

During this thesis, nine combinations of smoothing scale and correction factor values were tested (**Appendix 1**). Tested values for smoothing scale were 1.3488, 3 and 5, where 1.3488 is the default setting. Due to the partial overlapping of polydisperse droplets during imaging, the intensity of fluorescence emission from Alexa dye may vary across different parts of the droplets. Higher smoothing values can even out these differences and enable better polydisperse droplet detection, thus the other two tested values were 3 and 5. As for the correction factor, values of 0.4, 0.8 and 1.0 were tested, where 1.0 is the default setting. Having more lenient values prevents cutting off part of droplets due to possible uneven Alexa dye distribution in droplets, which is why the correction values of 0.8 and 0.4 were tested.

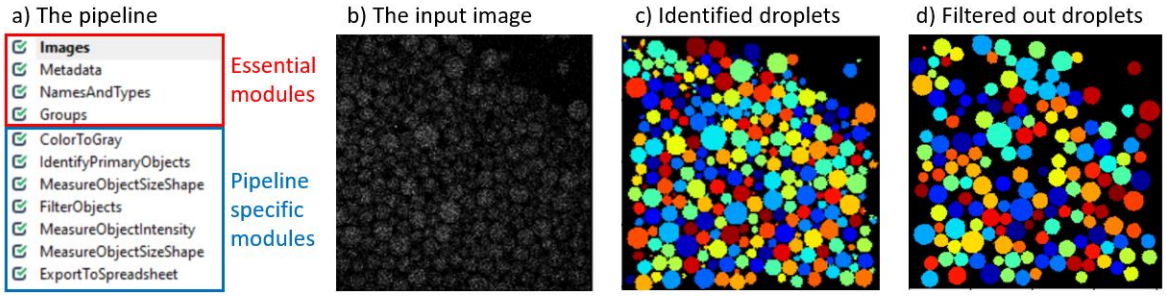

Figure 12. a) Used pipeline in CellProfiler™ in the MSc thesis by Fenella Lucia sulp. With the red box are marked essential input modules and with the blue box are brought out all the additional modules, which are specific to every pipeline. b) Image that will go as an input into CellProfiler™. c) The identified droplets after the first *IdentifyPrimaryObjects* module.

d) Unsuitable droplets are filtered out in *FilterObjects* module. Filtering is based on eccentricity and solidity of droplet area.

To make sure that the results are valid, accuracy was calculated using formula in **Figure 11**:

1) True positive (TP) – there is a droplet and CellProfiler™ finds it
2) False negative (FN) – there is a droplet, but CellProfiler™ cannot find it
3) False positive (FP) – there is no droplet, but CellProfiler™ counts something as a droplet

In that instance there could be no true negative, as it is not possible to count non-existing droplets, there is only background.

3.3 Measurement of bacterial viability

For the bacterial viability, the pipeline includes the *MeasureObjectIntensity* module. If the measured intensity is higher than 0.025, then the droplets will be classified as positive (viable). The fraction of positive droplets is always found by dividing the total amount of positive droplets with the total amount of all detected droplets in each respective sample (i.e each antibiotic concentration). Lastly, data will be normalized, which means that the control group will have a value of one (its fraction of positive droplets being divided by itself). Fraction of positive droplets from all other samples will then be divided by the fraction of positive droplets from control sample, resulting in overall values more comparable to other experiments.

To get the needed data for measuring bacterial viability in polydisperse droplets with and without microplastic, an additional *IdentifyPrimaryObjects* module, which identifies microplastic particles, is important for later differentiation between the two different types of droplets. After detecting all microplastics, the pipeline can connect droplets with the specific microplastic particles that are inside the droplet (*RelateObjects* module). During *FilterObjects* module all the droplets are separated into two categories (i) droplets with microplastic, and (ii) droplets without microplastic. Additionally, bacterial viability was found in control experiment, which was a separate experiment with polydisperse droplets that did not include microplastic particles.

3.4 Measurement of autoaggregation

Module *MeasureTexture*

To analyse autoaggregation in polydisperse droplets, *MeasureTexture* module was chosen because based on the texture values, the droplets can be classified into different growth groups, which are no bacterial growth (**Figure 13.a**), homogeneous growth (**Figure 13.b**) and aggregated growth (**Figure 13.c**). *MeasureTexture* module analyses the texture of images and objects, generating numerical measurements to characterize their roughness or smoothness. The number of gray levels the images were binned into was 256, which is the maximum possible value. More levels give more detailed information about the image; however, it also slows down the speed of processing.

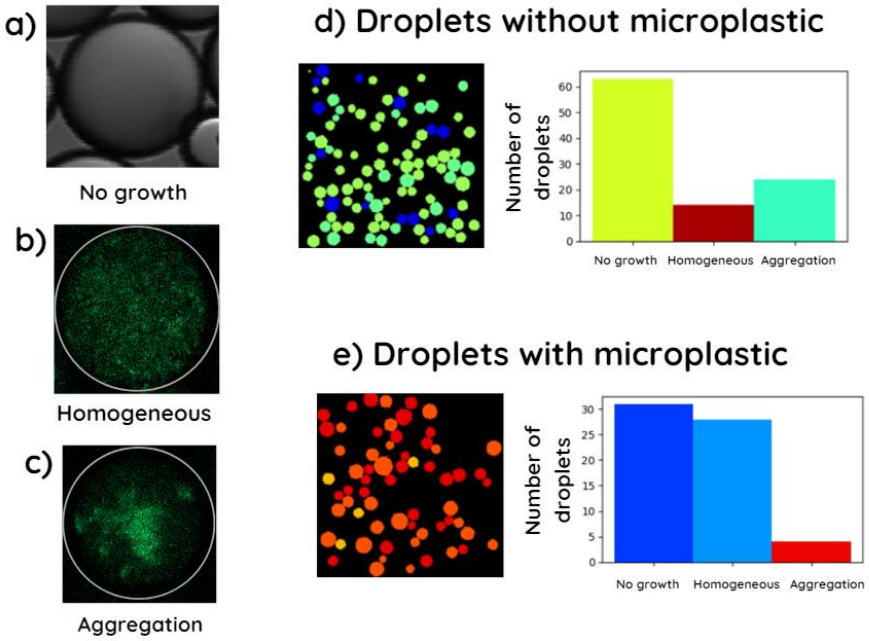

Figure 13. Output from CellProfiler™ after ClassifyObjects module and difference between bacterial growths. The diagrams show how the droplets are categorized (which growth group). The image next to diagram shows which droplets were used. The colours have no meaning since they are randomly chosen by CellProfiler™. The top images show how homogeneous growth, where the green intensity is smooth, differs from aggregated growth, which has spots with higher intensity.

MeasureTexure calculates thirteen measurements. For this study, five of those were tested:

1) AngularSecondMoment – measures homogeneity of image, where higher value indicates similar initensity and value of one means uniform image
2) Variance – measures the variation of intensity values, where the value of zero means uniform intensity
3) InverseDifferenceMoment – measures the image contrast, where homogeneous images have higher values
4) SumVariance – measures the variance of the normalized grayscale image in the spatial domain
5) DifferenceVariance – measures the image variation in a normalized co-occurrence matrix

The texture scale is the distance between correlated intensities in the image, in pixel units. It is recommended to use smaller scale than the object's size, otherwise the measurement is not accurate. During this study, three different texture scales were tested – 1, 3 and 10. The smallest scale is 1, 3 is the default and 10 was chosen from the diameter results. Since the texture scale must be significantly smaller than the droplets, the average of the smallest droplets, which is 100 pixels, is divided by ten (**Appendix 2**).

To analyse one data set:

1) CellProfiler™ exported in total of four values about one measurement method, which are the different directions the neighbouring pixel is comparing to.
2) The average of these four values was found.
3) The average values were sorted from the lowest to the highest value.

4) The data was plotted onto graphs to see whether three separate groups can be distinguished: (i) empty droplets, (ii) homogeneous growth of bacteria in droplets, and (iii) aggregated growth of bacteria in droplets.

In total there were fifteen sets of data needed to be analysed – each chosen measurement with three different texture scale values.

Module *ClassifyObjects*

Based on the texture values and set threshold, *ClassifyObjects* module classifies objects into different given categories. The separating bin values were 80 and 390 pixels, which were found from the histogram (**Appendix 3**). This means that droplets with values lower than 80 are categorized as no growth, droplets with values between 80 and 390 are categorized as homogeneous growth and droplets with values over 390 are categorized as autoaggregation (**Figure 13.d,e**). The output of *ClassifyObjects* module shows, which droplets contain microplastic (**Figure 13.e**) and their location on the image, and the same with droplets without microplastic (**Figure 13.d**). The module also shows diagrams of how many droplets belong to different category groups (no growth, homogeneous or aggregated) (**Figure 13.d,e**).

For the calculations, aggregated growth groups are needed from *ClassifyObjects* module. The fraction of droplets with aggregated bacteria growth is always found by diving the total amount of droplets containing autoaggregation with the total amount of all detected droplets in each respective sample (in this thesis antibiotic concentration). Lastly, the fraction of droplets with aggregated bacteria growth will then be divided by the fraction of aggregated bacteria growth of control sample, resulting in overall values more comparable to other experiments.

4. RESULTS AND DISCUSSION

The main aim of this thesis was to develop an image analysis pipeline to investigate the impact of microplastic to bacterial aggregation. The logic of the final developed pipeline is following:

1) The polydisperse droplets are imaged as a monoloayer in red, green, and bright-field channels (**Figure 14.1**).
2) The bright-field image will go through ilastik, which detects the microplastic particles and exports prediction files, where pixels belonging to microplastic particles are white, while pixels belonging to everything else are dark (**Figure 14.2**).
3) As an input to CellProfiler™, the user inserts all the image formats and the prediction of microplastic from ilastik (**Figure 14.3**).
4) CellProfiler™ then goes through the developed pipeline and exports .csv file results, which can be further analysed, for example in Excel (**Figure 14.4**).

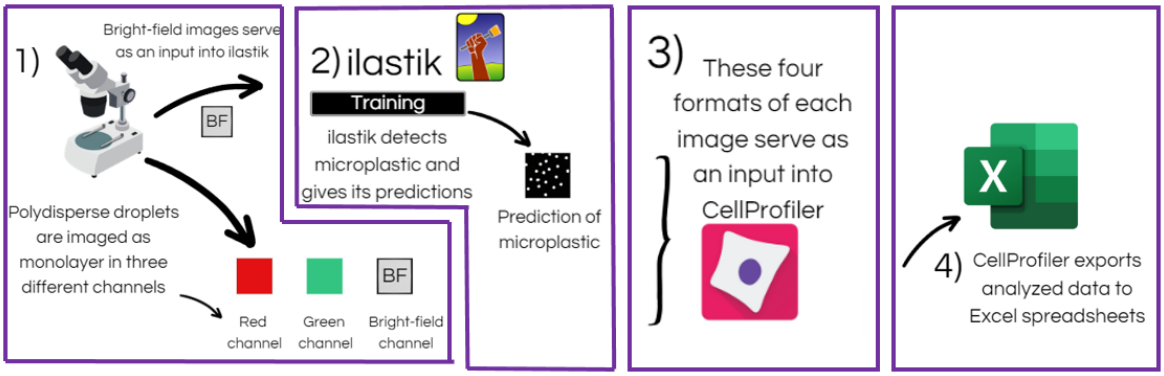

Figure 14. The journey from imaging the polydisperse droplets to getting data for further analysis.

The final pipeline in CellProfiler™ has eleven modules in addition to the four essential ones (**Figure 15.b**). First, it identifies all the droplets then all the microplastic particles (*IdentifyPrimaryObjects* module). After identifying objects, it will measure the size of the droplets (*MeasureObjectSizeShape* module) and later filters out droplets that do not fit the set criteria (*FilterObjects* module). When there are only wanted droplets, the pipeline will connect droplets with microplastic particles (*RelateObjects* module) and filters droplets into to two groups – droplets with microplastic and droplets without microplastic (*FilterObjects*). Next will be texture (*MeasureTexture* module), intensity (*MeasureObjectIntensity* module) and again size (*MeasureObjectSizeShape* module) measured. Before exporting results, droplets with and without microplastic will be categorised into three different bins – no bacterial growth, homogeneous growth, and aggregated growth (*ClassifyObjects* module).

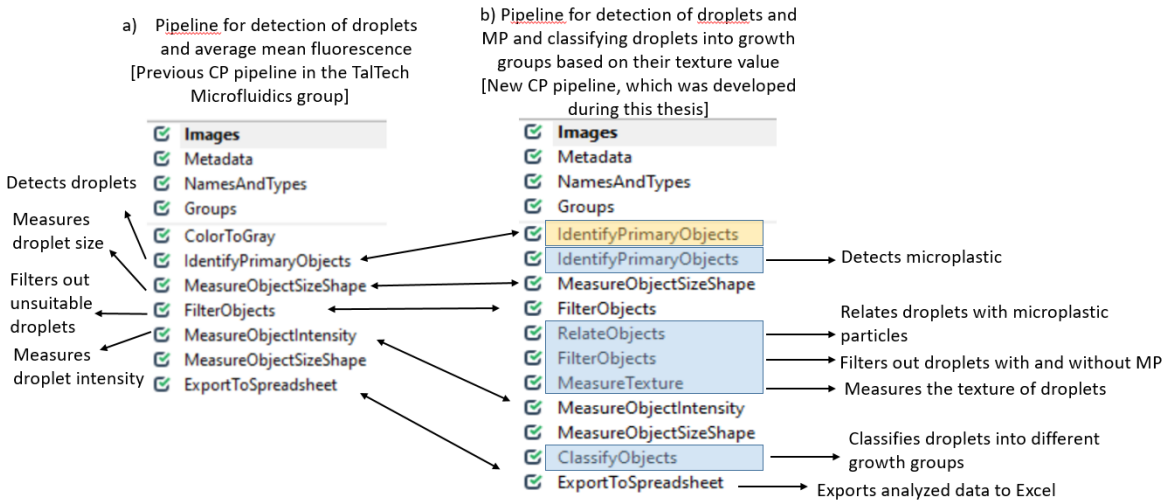

Figure 15. a) Used pipeline in CellProfiler™ from the MSc thesis by Fenella Lucia Sulp for detecting droplets and finding the average mean fluorescence. b) Finalized pipeline in CellProfiler™ for detection of droplets and microplastic and finding autoaggregation. With yellow is marked modified module and with blue are marked added modules.

Overall, the developed pipeline can help to investigate the impact of microplastic to bacterial aggregation. Due to CellProfiler™ not analyzing bright-field images well, usage of two software is necessary but make analyzing more difficult and time consuming. *MeasureTexture* module can be improved by exploring the two measurements SumVariance and Variance with more data sets. In this study, SumVariance was the best option, but more analysis is needed in the future to be sure.

4.1 Detection of microplastic

The first specific sub-aim was the detection of microplastic inside polydisperse droplets. The software ilastik detected all the microplastic particles and exported the prediction of microplastic acceptable for further analysis in CellProfiler™. While working with ilastik, there are two major checkpoints before getting the final prediction. First one is training (**Figure 16.b**), where the user manually marks with different labels what needs to be classified and applies appropriate thresholding. During training, it was decided to move forward with smoothing values 2 - 1.5 and threshold values 0.8-0.7, since it gave the best results. For identifying microplastic in CellProfiler™, threshold smoothing scale is 1.3488 and correction factor is set to 1, which are the default settings.

The second checkpoint is after training part (**Figure 16.c**), where the software gives out initial result. After the user checks the correctly identified objects and is overall satisfied with the output, the final prediction can be exported (**Figure 16.d**). The exported predictions from ilastik show (i) all the detected microplastic particles and (ii) background, which is all black (**Figure 16.d**). Also having accuracy of 93.40% with no false negatives indicate that ilastik was trained well (**Figure 16**).

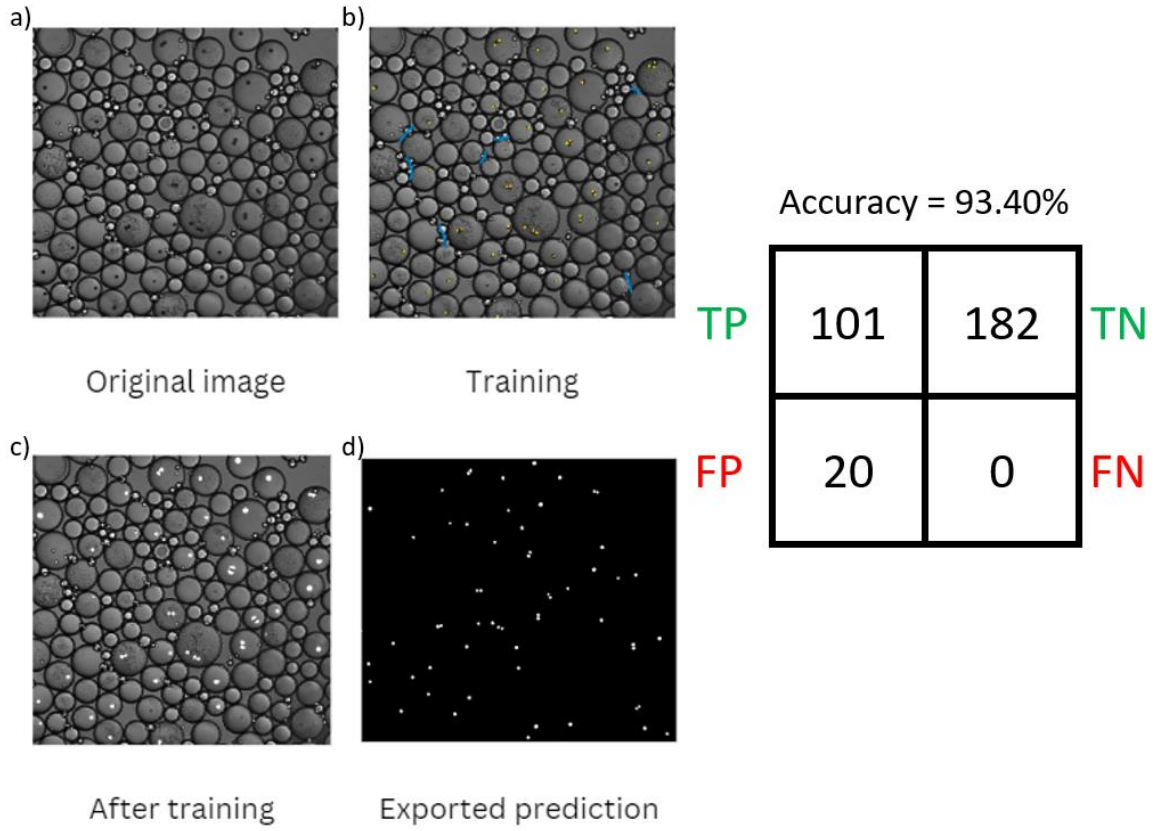

Figure 16. Different stages of using ilastik. a) First is the original image, which goes as an input. b) This image is during training with yellow and blue labels marking different objects. c) Then comes after training part, where ilastik shows what it has identified, and the user marks correct and incorrect results. d) Last image is the exported prediction of microplastic that will go into CellProfiler™. Calculated accuracy came to 93.4%.

Detection of microplastic via ilastik was successful, as the output files were suitable for further input and overall analysis in CellProfiler™. If wanted, ilastik can be trained with more images to get even higher accuracy. The more it is trained, the less it confuses non microplastics with real microplastic particles. However, more training also requires more manual labour of the trainee and cannot always guarantee a better outcome.

4.2 Optimization of droplets detection in CellProfiler™

The second specific sub-aim was to optimze the detection of polydisperse droplets. It was done by finding the diameter range of wanted droplets and the threshold-smoothing combination in *IdentifyPrimaryObjects* module. The first parameter was the objects diameter, which was found when measuring the droplets by hand (**Figure 17**). From the diameter measurements, it was chosen that the setting “typical diameter of objects in pixel units” should be 20 to 400 pixels. The second crucial parameter is the smoothing – threshold combination. From the nine different combinations tested, the threshold smoothing scale was set to 3 and threshold correction factor was set to 0.8 for identifying polydisperse droplets (**Appendix 1**). Given the few missed droplets and only one wrongly identified object, the accuracy came to 88.59%, which again was acceptable (**Figure 17**).

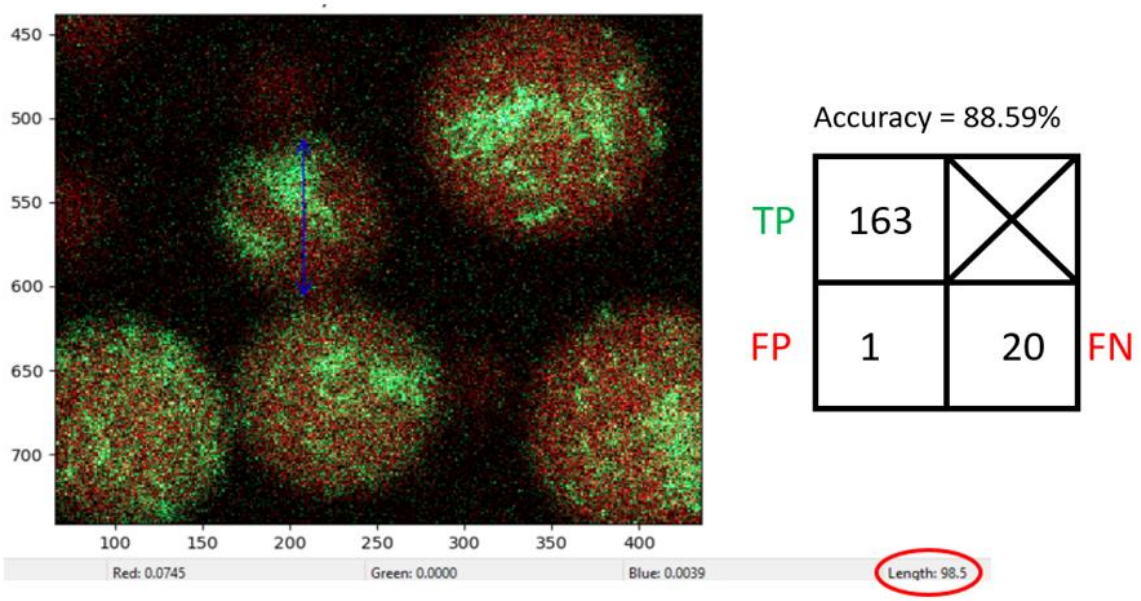

Figure 17. Example of measuring the smallest droplet on an image, which has diameter of 98.5 pixels (= 61.46 µm). The accuracy for detecting polydisperse droplets was 88.59%.

The key to optimizing polydisperse droplet detection is in *IdentifyPrimaryObjects* module. In this study three key module features were tested. To improve the detection even more, other settings in this module could also be evaluated. Polydisperse droplets are harder to analyse because of their inconsistencies in behaviour due to their size variations and their likelihood of overlapping during imaging (imaging slide chamber height is 100 µm). The detection depends also on image quality. The contrast between the droplets and background becomes harder to distinguish the drier droplets are. During imaging it is important to have enough oil mixed with droplets to ensure that droplets do not start drying out during the imaging process.

4.3 Antibiotic susceptibility in the presence of microplastic

The third specific sub-aim was to compare viability in polydisperse droplets with microplastic versus without microplastic. Viability of bacteria was higher in droplets with no microplastic. To calculate viability (i) sum of positive and sum of total droplets were found, then (ii) the respective sums were divided to find the fraction of positive droplets. For making the graph, normalized data was used (**Appendix 4**). In the graph, antiobiotic concentration is in the X-axis and bacterial viability is in the Y-axis. Results that are shown in green are from droplets that do not contain microplastic particles and result in orange shows the bacterial viability in droplets with microplastic. It appears that the presence of microplastic decreases bacterial viability (**Figure 18**).

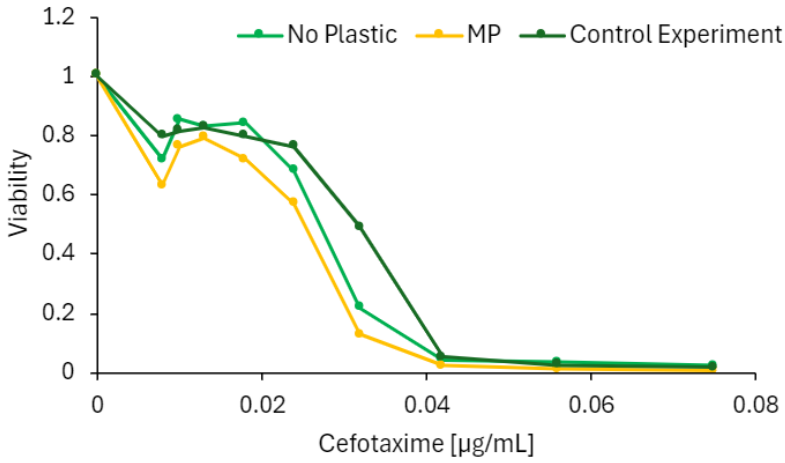

Figure 18. The comparison of bacterial viability in the presence of cefotaxime with microplastic versus without microplastic. Control experiment is done by using polydisperse droplets without any microplastic.

When comparing the results from the control experiment (a separate experiment without any microplastic included) versus the main experiment, where some droplets had and some did not have microplastic particles in them, it can be concluded that they all have a similar trendline. The two datasets (**Figure 18, light and dark green data**), which consist only of droplets without microplastic particles, have more similar values, which is logical. This further indicates that the developed pipeline gives out accurate data.

4.4 Antibiotic susceptibility in the presence of microplastic

The fourth specific sub-aim was to compare bacterial aggregation in polydisperse droplets with microplastic versus without microplastic. Autoaggregation of bacteria was higher with sample that did contain microplastic particles. Before calculating the bacterial aggregation, first it was crucial to know how to measure the texture of droplets. In this study, five different texture measurements were tested. After consideration, it was decided to move forward with SumVariance. For example, compared to InverseDifferenceMoment, it was clear that SumVariance could distinguish between empty droplets, homogeneous growth, and autoaggregation, whereas InverseDifferenceMoment could only distinguish between empty droplets and droplets with bacteria growth (**Figure 19**). The same comparison was done by a master student Merili Saar, who obtained similar results. During this cooperation, it was decided to continue with SumVariance.

As for the texture scale, from the three tested options 10 was chosen, because it separated needed three groups most noticeably. All the options were very similar, but when taking a closer look, the difference between homogeneous growth and aggregated growth groups is a little bit bigger with texture scale of ten (**Appendix 5**).

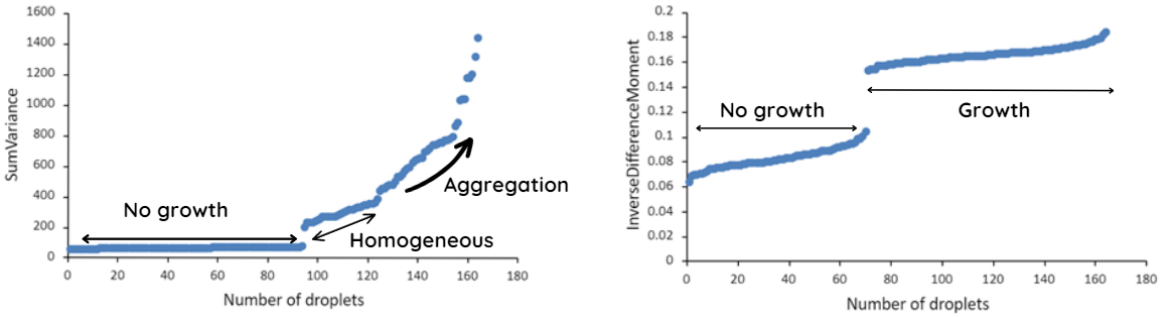

Figure 19. Comparison of two measuring methods. On the left is SumVariance, which enables categorization of droplets with no growth, homogeneous or aggregated growth. On the right is InverseDifferenceMoment, which has only one „jump", so categorization of homogeneous versus aggregate growth is not possible.

In the graph, antiobiotic concentration is in the X-axis and autoaggregation is in the Y-axis. If only looking at the datasets from polydisperse droplets with and without microplastic particles (**Figure 20, blue and light green data**), it seems as if the presence of microplastic increases autoaggregation in droplets. Series, which is made from the control data without any microplastic particles (**Figure 20, dark green data**), shows similar overall trendline of autoaggregation first increasing but soon decreasing with higher cefotaxime concentrations. Nevertheless, the control experiment autoaggregation dataset values do not match with the "No Plastic" dataset values, being even higher than values for the "Microplastic" dataset (**Figure 20**).

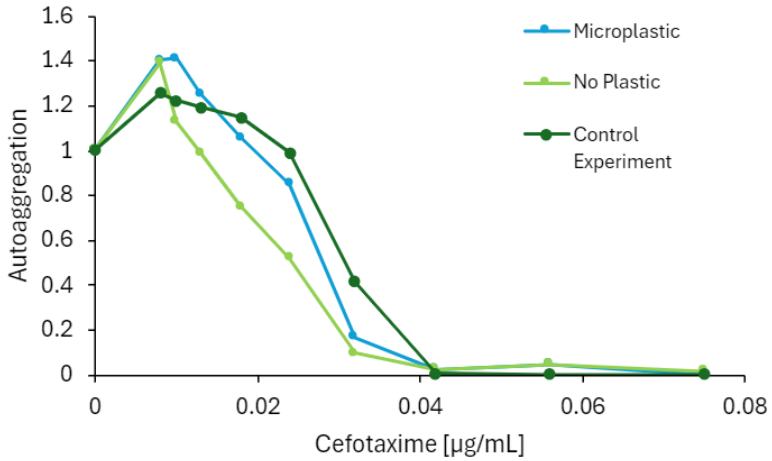

Figure 20. The comparison of autoaggregation in the presence of cefotaxime in droplets with microplastic versus without. Control experiment is done by using polydisperse droplets without any microplastic.

Knowing the accuracy of detection, it can be said that the output from the developed pipeline in this thesis is more precise than the previously used pipeline in the thesis of Fenella Lucia Sulp [37]. To get a deeper understanding of the relationship between autoaggregation and microplastic, more testing is needed, yet this pipeline is suitable for enabling aggregation analysis in droplets. It will be used in the BSc thesis by Triini Olman and it is fitting to use the pipeline in any other projects related to microplastic particles and aggregation. To improve this pipeline, more of the different settings in *IdentifyPrimaryObjects* module should be tested so see if it is possible to make the identification even more accurate. *MeasureTexture* module should be tested more thoroughly with the texture measurements SumVariance and Variance, to see which measurement is more fitting. To get even more accurate results, the testing should be done with better quality images. It is important that

the droplets are not dried out nor overlapping in the imaging chamber. It should be considered to do the testing with monodisperse droplets, since the images have usually better quality and overall they are easier to analyse. For further development, instead of ilastik, it is worth try to use some other software, since ilastik can be very time consuming and may not work on every computer. The software ilastik requires a 64-bit operating system and at least 8 GB of RAM (random access memory), but for smooth interaction at least 32 GB of RAM is needed [18].

ABSTRACT

Polydisperse droplets, which contain two immiscible liquids, give a chance to make small-scale experiments, while not needing any expensive equipment nor trained staff. To analyse made droplets, there have been developed different software, from which some are demanding programming skills. Fortunately, there are also more user-friendly image analysis software available. These applications are providing easy access to guides and manuals to help new users.

The main purpose of this thesis was to develop an image analysis pipeline to investigate the impact of microplastic to bacterial aggregation. The sub-aims were (i) to detect microplastic inside polydisperse droplets; (ii) to optimize the detection of polydisperse droplets; (iii) to compare the bacterial viability in polydisperse droplets with versus without microplastic; (iv) to compare the bacterial aggregation in polydisperse droplets with microplastic versus without microplastic.

The final pipeline uses software CellProfiler™ and ilastik. Images from bright-field channel serve as an input to ilastik, which exports predictions of microplastic. CellProfiler™ requires four images formats (red channel, green channel, bright-field channel, and prediction of microplastic) as an input. The final pipeline in CellProfiler™ has eleven modules added to the four essential ones. After going through the pipeline, the software exports .csv file results.

For the detection of microplastic, the software ilastik was trained. Most suitable correction factor and smoothing scale was found and in the end, it had 93.4% accuracy. To optimize detection of polydisperse droplets, diameter distribution was measured and different thresholds were tried. The typical diameter of objects in pixel units was set to 20 and 400 and threshold smoothing scale was settled to 3 and threshold correction factor was left to 0.8. The accuracy of droplet detection came to 88.59%.

Bacterial viability was higher in droplets without microplastic. This result was supported by the control experiment, which did not include microplastic particles. Bacterial aggregation was higher in droplet with microplastic. However, this result was not backed up by the control experiment, since its dataset values were even higher than the values of droplets with microplastic. Bacterial growth was classified based on their texture values into three groups – no growth, homogeneous growth, and aggregated growth. In conclusion, the analyses hint that microplastic has a decreasing effect on bacterial viability. However, bacterial aggregation needs more investigation with better quality images. The developed pipeline works and can be used for further research.

KOKKUVÕTE

Emulsioon koosneb kahest segunematu vedeliku faasist, milleks võib olla näiteks vesi ja õli. Emulsiooni tüüpe on erinevaid, kuid antud töös on kasutatud vesi-õlis tilkasid. Kasutades tilkasid katseklaasidena, saab kokku hoida reagentide kulu ja vähendada toksilisi jäätmeid. Monodispersed tilgad on sama läbimõõduga ning nende tootmiseks on välja töötatud erinevaid kanali disaine. Kuigi monodisperseid tilkasid on kergem uurida, nõuab nende tootmine erilisi seadmeid ning koolitatud personali. Polüdispersed tilgad seevastu on küll suuruselt erinevad, kuid nende tegemiseks ei ole vaja erilist seadmeid, tänu millele on seda võimalik teha igas laboris. Tehtud tilkade analüüsimiseks on välja töödeldud tarkvarasid, millest mõned vajavad teadmisi programmeerimises. Siiski on saadaval ka kasutajasõbralikumaid tarkavarasid nagu CellProfiler™, ilastik, QuPath ja ImageJ. Need rakendused pakuvad uutele kasutajatele lihtsat juurdepääsu juhenditele.

Tänapäeval on suureks probleemiks plastik, mis ei ole biolagunev, vaid laguneb mikroplastikuks ja nanoplastikuks. Mikroplastiku reostusel on negatiivne mõju inimese tervisele, tekitades erinevaid haigusi sattudes vereringesse. Mikroplastiku osakesi leidub meie toidus, õhus ja vees, mistõttu tarbivad inimesed nädalas kuni 5 grammi mikroplastikut. Antimikroobne resistentsus (AMR) on mikroobide suutelisus muutuda vastupanuvõimeliseks antibiootikumidele. Seetõttu on haiguse ravi raskendatud või üldsegi võimatu. Mikroorganismide võime kinnituda pinnale loob biokile. Üks esimesi samme biokile moodustumisel on agregatsioon ehk bakterid koonduvad kokku.

Käesoleva töö põhiliseks eesmärgiks oli pildianalüüsi töövoo arendamine mikroplastiku mõju uurimiseks bakterite agregatsioonile. Alaeesmärkideks olid (i) mikroplastiku tuvastamine polüdispersetes tilkades; (ii) polüdispersete tilkade tuvastamise optimeerimine; (iii) võrrelda bakterite elulisust polüdispersetes tilkades mikroplastikuga versus mikroplastikuta; (iv) võrrelda bakterite agregatsiooni polüdispersetes tilkades mikroplastikuga versus mikroplastikuta.

Lõplik töövoog kasutab tarkvarasid CellProfiler™ ja ilastik. ilastikult saab mikroplastiku ennustuse, mis sisestatakse koos kolme teise pildiformaadiga tarkvarasse CellProfiler™. Lõplik töövoog CellProfiler™ tarkvaras sisaldab lisaks kohustuslikule neljale moodulile veel ühtteistkümmet moodulit. Pärast töövoo läbi töötamist, ekspordib tarkvara .csv failina tulemused.

Mikroplastiku tuvastamiseks tuli ilastikut treenida. Leiti kõige täpema tulemuse andvad sätted. Arvutades saadi 93,4% täpsus, milles ükski mikroplastiku osa ei jäänud tuvastamata. Polüdispersete tilkade tuvastamise optimeerimiseks mõõdeti kõige suuremate ja väiksemate tilkade diameetreid ning lisaks prooviti erinevaid läveväärtusi. Lõpuks määrati tüüpiliseks objektide diameetriks vahemiku 20 ja 400 pikslit ning läve silumise skaalaks pandi 3 ja läve parandusteguriks jäeti 0,8. Tilkade tuvastamise täpsuseks arvutati 88,59%.

Bakterite elulisus oli kõrgem tilkades, mis ei sisaldanud mikroplastikut. Seda tulemust kinnitas ka kontrollkatse, mis ei sisaldanud üldse mikroplastikut. Bakterite agregatsioon oli kõrgem tilkades, kus oli ka mikroplastiku osakesi. Siiski, seda tulemust ei kinnitanud kontrollkatse, mille väärtused olid isegi suuremad, kui mikroplastikuga tilkade väärtused. Bakterite kasv jaotati tekstuuri väärtuste alusel kolme gruppi – tühjad tilgad, homogeenne kasv ja agregatsioon. Kokkuvõttes, tehtud analüüsid vihjavad asjaolule, et mikroplastikul on mõju bakteri elulisusele. Siiski baketri

agregatsioon vajab edasist uurimist, kasutades parema kvaliteediga pilte. Arendatud töövoog töötab ning seda saab kasutada edasistes uuringutes.

Acknowledgements

I would like to express my sincere gratitude to my supervisors, Simona Bartkova and Ott Scheler, for their support and expertise throughout my study. Their guidance, patience, and motivation helped me at every step of the research and writing process of the thesis.

I would also like to thank Immanuel Sanka for his assistance with using CellProfiler™, and Merili Saar for support and pleasant cooperation.

REFERENCES

[1] R. Thakur, A. Sharma, P. Verma, and A. Devi, “A Review on Pharmaceutical Emulsion,” *Asian Journal of Pharmaceutical Research and Development*, vol. 11, no. 3, 2023, doi: 10.22270/ajprd.v11i3.1181.

[2] S. Mashaghi, A. Abbaspourrad, D. A. Weitz, and A. M. van Oijen, “Droplet microfluidics: A tool for biology, chemistry and nanotechnology,” *TrAC - Trends in Analytical Chemistry*, vol. 82. Elsevier B.V., pp. 118–125, Sep. 01, 2016. doi: 10.1016/j.trac.2016.05.019.

[3] B. Li *et al.*, “Droplets microfluidics platform—A tool for single cell research,” *Frontiers in Bioengineering and Biotechnology*, vol. 11. 2023. doi: 10.3389/fbioe.2023.1121870.

[4] S. A. Byrnes, E. A. Phillips, T. Huynh, B. H. Weigl, and K. P. Nichols, “Polydisperse emulsion digital assay to enhance time to detection and extend dynamic range in bacterial cultures enabled by a statistical framework,” *Analyst*, vol. 143, no. 12, pp. 2828–2836, Jun. 2018, doi: 10.1039/c8an00029h.

[5] H. Jasmina, O. Džana, E. Alisa, V. Edina, and R. Ognjenka, “Preparation of nanoemulsions by high-energy and lowenergy emulsification methods,” in *IFMBE Proceedings*, 2017. doi: 10.1007/978-981-10-4166-2_48.

[6] A. Kalantarifard, E. Alizadeh-Haghighi, and C. Elbuken, “A microfluidic droplet system for ultra-monodisperse droplet generation: A universal approach,” *Chem Eng Sci*, vol. 261, 2022, doi: 10.1016/j.ces.2022.117947.

[7] S. Y. Teh, R. Lin, L. H. Hung, and A. P. Lee, “Droplet microfluidics,” *Lab on a Chip*, vol. 8, no. 2. Royal Society of Chemistry, pp. 198–220, 2008. doi: 10.1039/b715524g.

[8] S. A. Byrnes *et al.*, “Wash-Free, Digital Immunoassay in Polydisperse Droplets,” *Anal Chem*, vol. 92, no. 5, 2020, doi: 10.1021/acs.analchem.9b02526.

[9] S. A. Byrnes, T. C. Chang, T. Huynh, A. Astashkina, B. H. Weigl, and K. P. Nichols, “Simple Polydisperse Droplet Emulsion Polymerase Chain Reaction with Statistical Volumetric Correction Compared with Microfluidic Droplet Digital Polymerase Chain Reaction,” *Anal Chem*, vol. 90, no. 15, 2018, doi: 10.1021/acs.analchem.8b01988.

[10] Y. Xue *et al.*, “PddCas: A Polydisperse Droplet Digital CRISPR/Cas-Based Assay for the Rapid and Ultrasensitive Amplification-Free Detection of Viral DNA/RNA,” *Anal Chem*, vol. 95, no. 2, 2023, doi: 10.1021/acs.analchem.2c03590.

[11] I. Sanka, S. Bartkova, P. Pata, O. P. Smolander, and O. Scheler, “Investigation of Different Free Image Analysis Software for High-Throughput Droplet Detection,” *ACS Omega*, vol. 6, no. 35, pp. 22625–22634, Sep. 2021, doi: 10.1021/acsomega.1c02664.

[12] D. R. Stirling, M. J. Swain-Bowden, A. M. Lucas, A. E. Carpenter, B. A. Cimini, and A. Goodman, “CellProfiler 4: improvements in speed, utility and usability,” *BMC Bioinformatics*, vol. 22, no. 1, Dec. 2021, doi: 10.1186/s12859-021-04344-9.

[13] “CellProfiler Project.” Accessed: May 17, 2024. [Online]. Available: cellprofiler.org

[14] S. Bartkova, M. Vendelin, I. Sanka, P. Pata, and O. Scheler, “Droplet image analysis with user-friendly freeware CellProfiler,” *Analytical Methods*, vol. 12, no. 17, pp. 2287–2294, 2020, doi: 10.1039/d0ay00031k.

[15] Y. S. Lau, L. Xu, Y. Gao, and R. Han, “Automated muscle histopathology analysis using CellProfiler,” *Skelet Muscle*, vol. 8, no. 1, 2018, doi: 10.1186/s13395-018-0178-6.

[16] S. Berg *et al.*, “ilastik: interactive machine learning for (bio)image analysis,” *Nat Methods*, vol. 16, no. 12, pp. 1226–1232, Dec. 2019, doi: 10.1038/s41592-019-0582-9.

[17] C. Sommer, C. Straehle, U. Kothe, and F. A. Hamprecht, "Ilastik: Interactive learning and segmentation toolkit," in *Proceedings - International Symposium on Biomedical Imaging*, 2011. doi: 10.1109/ISBI.2011.5872394.
[18] "ilastik." Accessed: May 18, 2024. [Online]. Available: ilastik.org
[19] K. Moor *et al.*, "High-avidity IgA protects the intestine by enchaining growing bacteria," *Nature*, vol. 544, no. 7651, 2017, doi: 10.1038/nature22058.
[20] W. Menegas *et al.*, "Dopamine neurons projecting to the posterior striatum form an anatomically distinct subclass," *Elife*, vol. 4, no. AUGUST2015, 2015, doi: 10.7554/eLife.10032.
[21] A. A. Koelmans, P. E. Redondo-Hasselerharm, N. H. M. Nor, V. N. de Ruijter, S. M. Mintenig, and M. Kooi, "Risk assessment of microplastic particles," *Nature Reviews Materials*, vol. 7, no. 2. 2022. doi: 10.1038/s41578-021-00411-y.
[22] A. I. Osman *et al.*, "Microplastic sources, formation, toxicity and remediation: a review," *Environmental Chemistry Letters*, vol. 21, no. 4. 2023. doi: 10.1007/s10311-023-01593-3.
[23] S. Bartkova, A. Kahru, M. Heinlaan, and O. Scheler, "Techniques Used for Analyzing Microplastics, Antimicrobial Resistance and Microbial Community Composition: A Mini-Review," *Frontiers in Microbiology*, vol. 12. 2021. doi: 10.3389/fmicb.2021.603967.
[24] E. Christaki, M. Marcou, and A. Tofarides, "Antimicrobial Resistance in Bacteria: Mechanisms, Evolution, and Persistence," *Journal of Molecular Evolution*, vol. 88, no. 1. 2020. doi: 10.1007/s00239-019-09914-3.
[25] Y. Zhao, S. Liu, and H. Xu, "Effects of microplastic and engineered nanomaterials on inflammatory bowel disease: A review," *Chemosphere*, vol. 326. 2023. doi: 10.1016/j.chemosphere.2023.138486.
[26] V. K. Sharma, X. Ma, E. Lichtfouse, and D. Robert, "Nanoplastics are potentially more dangerous than microplastics," *Environmental Chemistry Letters*, vol. 21, no. 4. 2023. doi: 10.1007/s10311-022-01539-1.
[27] H. Lai, X. Liu, and M. Qu, "Nanoplastics and Human Health: Hazard Identification and Biointerface," *Nanomaterials*, vol. 12, no. 8. 2022. doi: 10.3390/nano12081298.
[28] K. Mattsson, E. V. Johnson, A. Malmendal, S. Linse, L. A. Hansson, and T. Cedervall, "Brain damage and behavioural disorders in fish induced by plastic nanoparticles delivered through the food chain," *Sci Rep*, vol. 7, no. 1, 2017, doi: 10.1038/s41598-017-10813-0.
[29] R. Kumar *et al.*, "Micro(nano)plastics pollution and human health: How plastics can induce carcinogenesis to humans?," *Chemosphere*, vol. 298, 2022, doi: 10.1016/j.chemosphere.2022.134267.
[30] ECDC, "Antimicrobial resistance surveillance in Europe 2022 - 2020 data," *WHO Regional Office for Europe/European Centre for Disease Prevention and Control*. 2022.
[31] G. Kapoor, S. Saigal, and A. Elongavan, "Action and resistance mechanisms of antibiotics: A guide for clinicians," *Journal of Anaesthesiology Clinical Pharmacology*, vol. 33, no. 3. 2017. doi: 10.4103/joacp.JOACP_349_15.
[32] "Cell Wall Synthesis Inhibitors: Examples, Inhibition, Resistance." Accessed: May 26, 2024. [Online]. Available: https://microbenotes.com/cell-wall-synthesis-inhibitors/#mechanisms-of-resistance
[33] "DNA Synthesis Inhibitors- Definition, Examples, Inhibition, Resistance." Accessed: May 26, 2024. [Online]. Available: https://microbenotes.com/dna-synthesis-inhibitors/
[34] "Protein Synthesis Inhibitors- Definition, Examples, Inhibition, Resistance." Accessed: May 26, 2024. [Online]. Available: https://microbenotes.com/protein-synthesis-inhibitors/

[35] R. M. Donlan, “Biofilms: Microbial life on surfaces,” *Emerging Infectious Diseases*, vol. 8, no. 9. 2002. doi: 10.3201/eid0809.020063.
[36] T. Trunk, H. S. Khalil, and J. C. Leo, “Bacterial autoaggregation,” *AIMS Microbiol*, vol. 4, no. 1, pp. 140–164, 2018, doi: 10.3934/microbiol.2018.1.140.
[37] F. L. Sulp, “Investigating effect of microplastic on antimicrobial resistance via droplet-based platform,” 2023.

Appendix 1

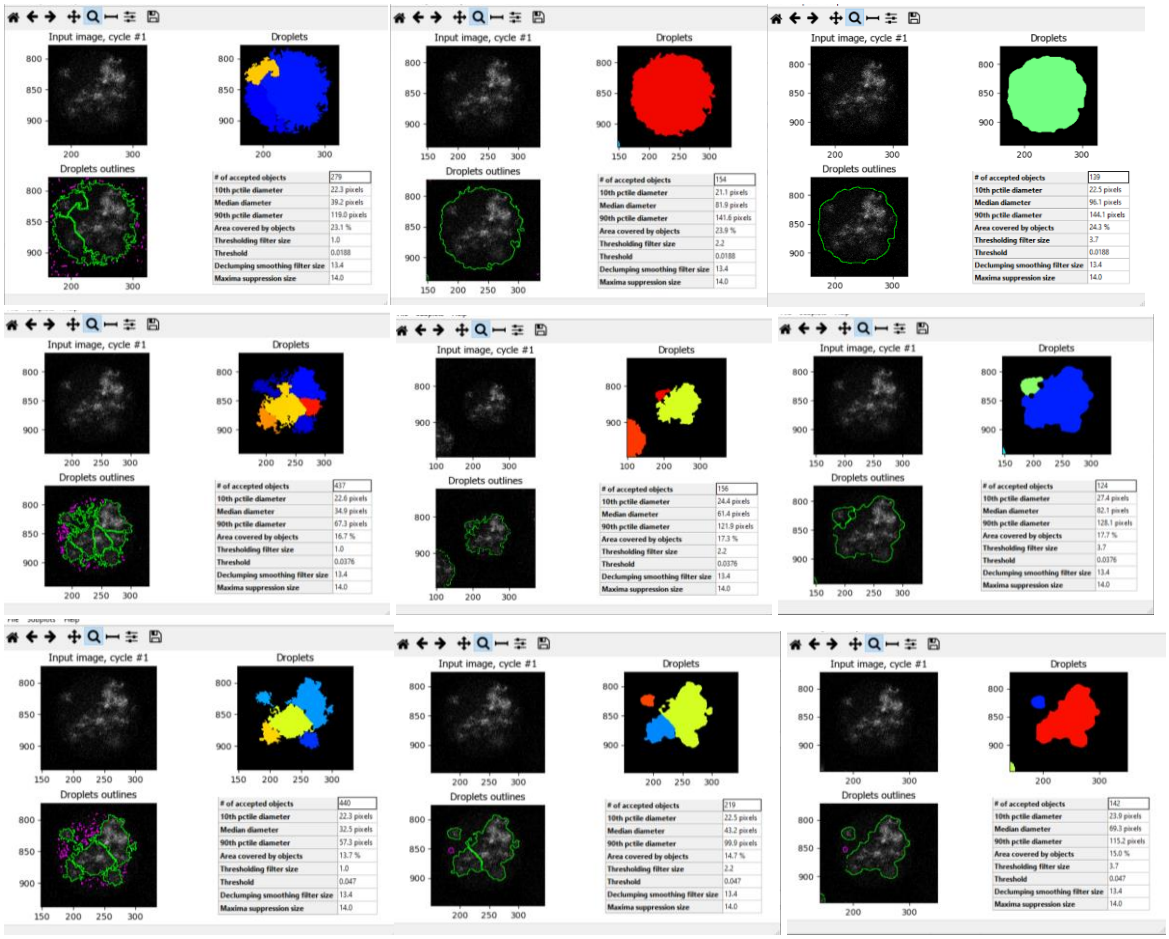

Appendix 1. Different smoothing scales and correction factors. From left to right, smoothing scales are 1.3488, 3 and 5. From top to bottom, correction factors are 0.4, 0.8 and 1.

Appendix 2

Droplet diameter in pixels

Droplet	smallest	biggest
Folder 11, image 1	149.8	402.1
Folder 12, image 2	120.9	408.5
Folder 13, image 3	137.6	337.1
Folder 14, image 1	124.8	263.5
Folder 15, image 2	83.8	275.3
Folder 16, image 3	71.8	252.5
Folder 17, image 4	98.5	282
Folder 18, image 1	74	337.1
Folder 19, image 2	79.9	372
Folder 9, image 5	92.3	190.4
Folder 1, image 30	102.1	465.8
Folder 2, image 22	87.4	247.1
Folder 3, image 8	79.1	322.6
Folder 4, image 28	95	266.3
Folder 5, image 6	82.1	187.2
Folder 6, image 4	85	251.6
Folder 7, image 4	96.3	275.3
Folder 8, image 2	92.4	227.7
Folder 10, image 7	123	270.6

Smallest	71.8
Biggest	465.8

	Smallest	Biggest
Average	98.72632	296.5632

Appendix 2. Droplet diameter distribution. From each folder, one image was chosen. From that image was the smallest and biggest droplet found and its diameter measured. From all the measured droplets was brought up the smallest and biggest diameter found and also the average calculated.

Appendix 3

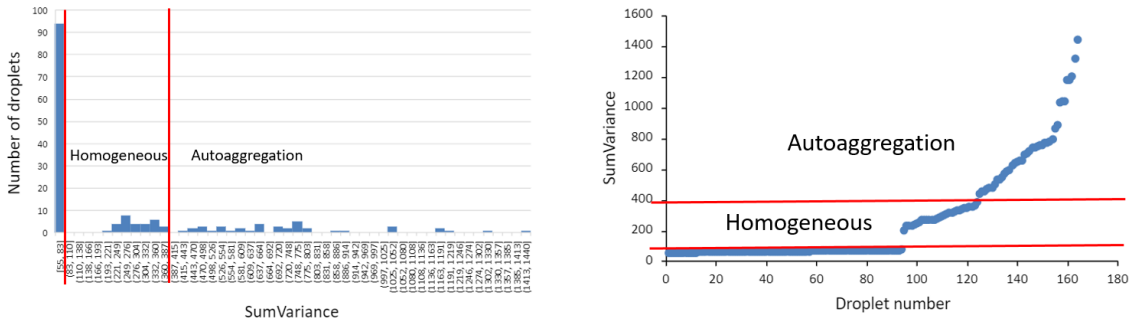

Appendix 3. On the left, histogram of SumVariance measurement to determine the separating threshold values for the bins. On the right, scatter chart of SumVariance values, which show the "jumps" between different growth groups.

Appendix 4

Sample	Sum of Positive	Sum of Total
1	15	1294
2	65	3563
3	78	3315
4	298	2311
5	1261	3131
6	1529	3070
7	1496	3040
8	1606	3175
9	1709	4023
10	1176	1981

Sample	Antibiotic concentration	Fraction of positive droplets	Normalized data
1	0.075	0.011591963	0.019526938
2	0.056	0.018243054	0.030730858
3	0.042	0.023529412	0.039635854
4	0.032	0.128948507	0.21721683
5	0.024	0.402746726	0.67843645
6	0.018	0.498045603	0.838969676
7	0.013	0.492105263	0.828963033
8	0.01	0.505826772	0.85207724
9	0.008	0.424807358	0.715598108
10	0	0.593639576	1

Sample	Sum of Positive	Sum of Total
1	3	655
2	7	957
3	15	945
4	64	631
5	276	608
6	414	724
7	544	863
8	444	731
9	499	991
10	1145	1432

Sample	Antibiotic concentration	Fraction of positive droplets	Normalized data
1	0.075	0.004580153	0.005728191
2	0.056	0.007314525	0.009147947
3	0.042	0.015873016	0.019851667
4	0.032	0.101426307	0.126849321
5	0.024	0.453947368	0.567731556
6	0.018	0.571823204	0.715153562
7	0.013	0.630359212	0.788361914
8	0.01	0.607387141	0.759631778
9	0.008	0.503531786	0.629744557
10	0	0.799581006	1

Appendix 4. Calculated fractions of positive droplets and normalized data, which was used to make graphs. Up is data from droplets without microplastic, down are the results from droplets with microplastic.

Appendix 5

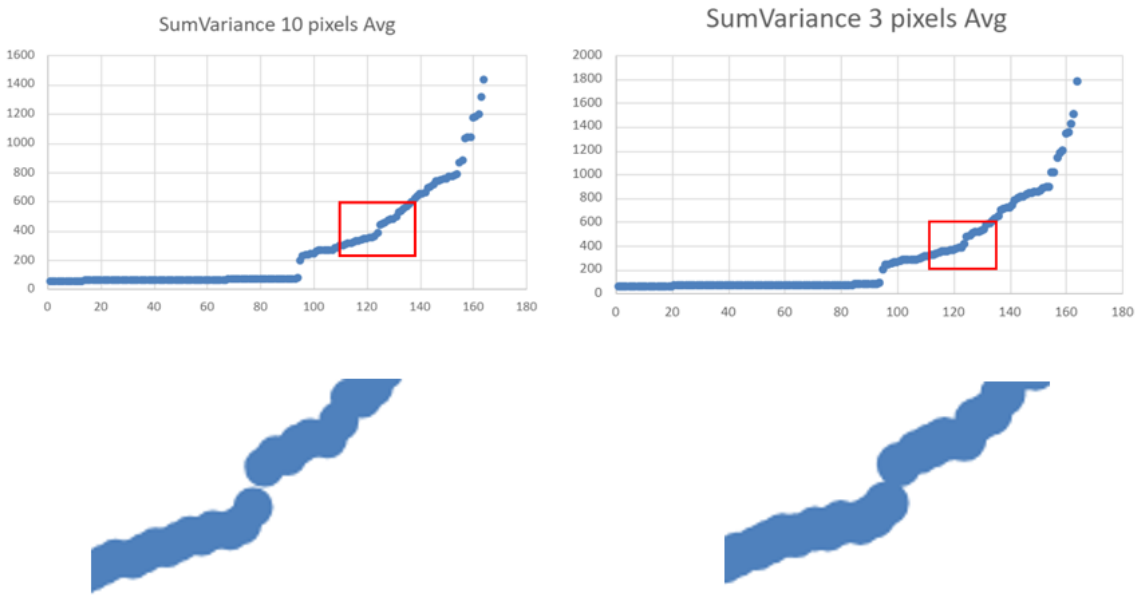

Appendix 5. Different tested pixel values. The clearest „jump“ between homogeneous growth and aggregated growth is on the left (10 pixels).

Lisa
rektori 07.04.2020 käskkirjale nr 1-8/17

Lihtlitsents lõputöö reprodutseerimiseks ja lõputöö üldsusele kättesaadavaks tegemiseks[1]

Mina Karoline Lindpere

1. Annan Tallinna Tehnikaülikoolile tasuta loa (lihtlitsentsi) enda loodud teose
Development of image analysis pipeline to investigate the impact of microplastic to bacterial aggregation

mille juhendajad on Simona Bartkova ja Ott Scheler,

1.1 reprodutseerimiseks lõputöö säilitamise ja elektroonse avaldamise eesmärgil, sh Tallinna Tehnikaülikooli raamatukogu digikogusse lisamise eesmärgil kuni autoriõiguse kehtivuse tähtaja lõppemiseni;

1.2 üldsusele kättesaadavaks tegemiseks Tallinna Tehnikaülikooli veebikeskkonna kaudu, sealhulgas Tallinna Tehnikaülikooli raamatukogu digikogu kaudu kuni autoriõiguse kehtivuse tähtaja lõppemiseni.

2. Olen teadlik, et käesoleva lihtlitsentsi punktis 1 nimetatud õigused jäävad alles ka autorile.

3. Kinnitan, et lihtlitsentsi andmisega ei rikuta teiste isikute intellektuaalomandi ega isikuandmete kaitse seadusest ning muudest õigusaktidest tulenevaid õigusi.

29.05.2024

[1] *Lihtlitsents ei kehti juurdepääsupiirangu kehtivuse ajal vastavalt üliõpilase taotlusele lõputööle juurdepääsupiirangu kehtestamiseks, mis on allkirjastatud teaduskonna dekaani poolt, välja arvatud ülikooli õigus lõputööd reprodutseerida üksnes säilitamise eesmärgil. Kui lõputöö on loonud kaks või enam isikut oma ühise loomingulise tegevusega ning lõputöö kaas- või ühisautor(id) ei ole andnud lõputööd kaitsvale üliõpilasele kindlaksmääratud tähtajaks nõusolekut lõputöö reprodutseerimiseks ja avalikustamiseks vastavalt lihtlitsentsi punktidele 1.1. jq 1.2, siis lihtlitsents nimetatud tähtaja jooksul ei kehti.*